Thermodynamics and Kinetics of Redox Switching of Polyvinylferrocene Films in Perchlorate Solutions

Stanley Bruckenstein,*,† Petr Krtil,§ and A. Robert Hillman‡

Department of Chemistry, State University of New York at Buffalo, Buffalo, New York 14260, and Department of Chemistry, University of Leicester, University Road, Leicester LE1 7RH, England

Received: March 11, 1998

Cyclic voltammetry was used to create nonequilibrium populations of different solvation and configurational states of partially oxidized polyvinylferrocene (PVF). Oxidation levels were established by scanning either from a fully reduced state to the desired oxidation level or from a fully oxidized state to the desired level. Coulostatic conditions were then established by opening the external circuit, and subsequent mass and potential changes were followed. The film's approach to equilibrium involves configurational changes within the polymer and simultaneous and subsequent solvent transfer. At very short times ($t \leq 0.2$ s) the approach to equilibrium is limited by both solvation and reconfiguration processes. For a short time afterward ($0.2 < t/\mathrm{s} < 1.0$) reconfiguration alone is rate limiting. At intermediate times ($1 < t/\mathrm{s} < 5$) both processes play comparable roles. At long times ($t > 5$ s) solvation is the controlling step. The electroactive polymer film does not completely reach equilibrium even after 1 h at open circuit as evidenced by continuous small mass changes. These mass changes are the result of water transfer between the polymer film and the bathing electrolyte. A scheme of cubes model rationalizes mechanistic pathways leading to equilibrium. In particular, the observed extrema in mass (solvent population) are predicted. The electrode potential, after 1 h at open circuit, shows nearly Nernstian dependence on the redox composition for film states produced by either anodic or cathodic cyclic voltammetric scans. These Nernst plots are displaced by only a few millivolts because only a weak Nernstian dependence on film water content exists. Films that are 50% oxidized exhibit a sub-Nernstian response with respect to the perchlorate concentration in the bathing solution under permselective conditions.

I. Introduction

Electroactive polymer modified electrodes became a subject of significant electrochemical interest in the late 1970s. Due to their useful properties and possible applications[1−4] many papers appeared that focused on the study of polymer modified electrodes' properties. The earliest model of a polymer modified electrode described it as a metal surface covered with a three-dimensional polymer network functionalized by homogeneously distributed, noninteracting redox centers. This model anticipated a simple Nernstian behavior of the redox polymer[1] and suggested that the thermodynamic properties of the redox polymer should be close to those of the monomeric redox couple in solution. However, "nonideal" behavior is generally to be expected.

The simple model usually fails to fit experimental data well. Evans et al. modified the simple model and introduced corrections for volume changes caused by redox switching and the mechanical energy connected with these changes.[5−7] Bard et al.[8,9] used a different model, assuming not one but a set of discrete $E°$ values to fit cyclic voltammetric data. Lang, Bacskai, and Inzelt[10] used a transmission line model based upon two double-layer capacitances at each boundary of the film to explain anomalies in impedance spectra. Hillman and Bruckenstein,[11,12] in a different approach, visualized the redox switching process as a sequence of three kinds of elementary steps: coupled electron/ion transfer, solvent transfer, and polymer reconfiguration. Each individual chemical step could occur before or after coupled electron/ion transfer and on the same or different time scales. To simplify the problem, they assumed that the totally oxidized and reduced polymer forms could exist in only two solvated and two configurational forms. They visualized these eight species as each existing at the corners of a cube. This "scheme of cubes" model in a 3-D space was used to interpret electrochemical quartz crystal microbalance (EQCM) data.

Whatever the correct kinetic model is, a thermodynamic basis is required to explain data for a system that has reached global equilibrium. However,[10,11] equilibrium may be attained very slowly. Predicting, a priori, the time for a given system to reach equilibrium is difficult;[13] also, what is evidence for the existence of equilibrium has not been stated clearly. In this paper, we define equilibrium as a state for which the electrode potential, charge, and mass are time invariant and independent of the way in which the oxidation level of the polymer has been established.

First we develop the scheme of cubes model as it applies to the equilibrium behavior of a reversible redox switching process. Second, we present experimental results for the transient potential behavior of PVF during partial redox switching and use the scheme of cubes model to rationalize our results. Third, we show this system's slow approach to thermodynamic equilibrium under open circuit (coulostatic) conditions.

† State University of New York at Buffalo.
‡ University of Leicester.
§ Permanent address: Petr Krtil, J. H. Heyrovsky Institute of Physical Chemistry, Dolejskova 3, 18223 Prague 8, Czech Republic.

S1089-5647(98)01468-0 CCC: $15.00
Published on Web 05/28/1998

II. Experimental Section

II.1. Chemicals. Methylene chloride (Fischer Scientific, ACS grade) was distilled over CaH_2 at atmospheric pressure. The fraction boiling at 37−39 °C was collected and stored under nitrogen atmosphere in the dark. Polyvinylferrocene (Polysciences, MW 50 000) was purified by reprecipitation.[14] Sodium perchlorate (Fischer Scientific, ACS grade), perchloric acid (Baker, ACS grade), and tetrabutylammonium perchlorate (TBAP, Kodak, 99%) were used as received. All solutions were prepared using Millipore MilliQ quality water and were deoxygenated by bubbling with nitrogen during all experiments.

II.2. Preparation of PVF Films. PVF films were prepared by electrochemical precipitation from 0.1 M TBAP/methylene chloride system.[13] Freshly prepared films were immediately rinsed with methylene chloride and dried in air. Between experiments, the PVF-coated electrodes were stored in aqueous 0.1 M $HClO_4$.

II.3. Instrumentation. All electrochemical experiments were done in a glass cell with two compartments, using a three-electrode potentiostat. A platinum wire, in a separate cell compartment, served as the auxiliary electrode. All potentials were measured and are given versus an aqueous saturated calomel electrode (SCE). The potentiostat was modified by a circuit that permitted the auxiliary electrode to be automatically disconnected from the circuit at a preset film charge level. A window detector monitored the voltage output of an analog integrator and opened the circuit when the desired film charge was reached.[14] Then, the charge state of the film was "frozen" by disconnecting the auxiliary electrode. Subsequent changes in the working electrode potential depended only on following chemical steps, namely, polymer reconfiguration and/or solvent transfer.[10]

The EQCM instrumentation has been described elsewhere.[15] AT cut, 10 MHz quartz crystals (International Crystal Manufacturing Co., Oklahoma City, OK) with evaporated gold layers were used. One gold layer acted as the working electrode. The electrochemically active geometric area of the electrode was 0.25 cm^2; the piezoelectric active area of the electrode was 0.22 cm^2. The output signals from the potentiostat and from the EQCM were recorded using a Keithley 500 series data acquisition system, connected to an IBM-PC. The acquisition rate was 256 points s^{-1} for the first minute and was 2 points s^{-1} afterward.

II.4. Potential and EQCM Measurements at Zero Current. A PVF modified gold electrode was held at 0.0 V for 1 h in the selected aqueous electrolyte. Then it was potential cycled at a scan rate of 50 mV s^{-1} between 0.0 and 0.6 V until steady-state cyclic I vs E and M vs E curves were attained. Usually ∼15 potential cycles were sufficient. The output signals of the potentiostat (E, I, Q) and of the EQCM (Δf) were simultaneously captured. After steady state was reached, the auxiliary electrode was automatically disconnected at a preselected charge level, typically 20, 40, 50, 60, or 80% oxidized. The oxidation level was determined from the charge, Q, passed and the charge required to oxidize the film completely, Q_{max}. Q_{max} was determined by integrating the current during a potential scan between 0 and +0.6 V while scanning at a rate of 50 mV s^{-1}. For the film we studied, $Q_{max} = 290\ \mu C$. Comparable results were obtained for other films having similar coverage. E and Δf continued to be recorded after disconnecting the auxiliary electrode.

Experiments were performed going from more oxidized to less oxidized charge levels, and vice versa. We denote "anodic scan data" as those obtained after disconnecting the auxiliary electrode while the potential was scanned to more positive values and "cathodic scan data" as those obtained while the potential was scanned to more negative values. Crystal impedance data show that the Sauerbrey equation may be used to convert Δf data to PVF film mass changes, ΔM, under the conditions used here.[16]

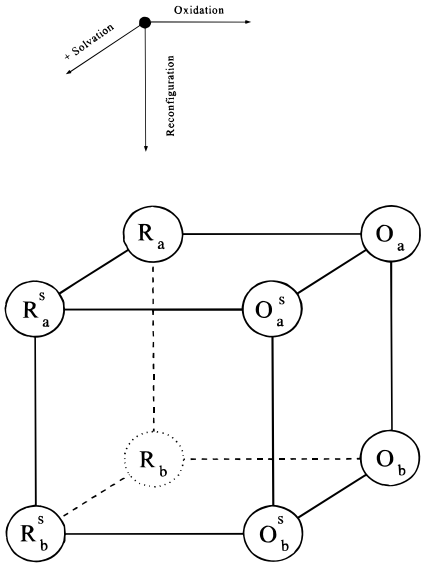

Figure 1. Insert: three-dimensional coordinate system for an electroactive polymer existing in different solvation and configuration states. Cube showing oxidized and reduced polymer solvation and configuration states.

III. Theoretical Section

III.1. Thermodynamics of the Cube. A rigorous interpretation of EQCM experimental data would demand considering the multiple redox, solvation, and configuration processes that might accompany oxidation or reduction of the PVF film. However, the accuracy of EQCM studies does not justify such a sophisticated approach. Consequently, we interpret our experimental results using a simplified model, the "scheme of cubes".

The insert in Figure 1 represents a rectangular coordinate system in which (electro)chemical transformations representing oxidation, solvation, and reconfiguration are assigned to the $+x$, $+y$, and $-z$ directions. The cube in Figure 1 shows the eight species in this model as existing at its corners. R designates a reduced polymer film species and O an oxidized species. Subscripts "a" and "b" show the two different configuration states, and the superscript "S" shows the more solvated state. The less solvated state has no superscript. This simple model requires us to consider only four redox couples, four solvation changes and four polymer reconfiguration processes.

III. 1.2. Standard Potential/Equilibrium Constant Relationships. The various interrelationships that exist between the different species are readily obtained. For notational simplicity in the following, we use Figure 2 as the scheme of cubes representation of the redox system. Species 1, 3, 5, and 7 correspond to the four reduced species, and species 2, 4, 6, and 8 correspond to the four oxidized species. The standard potentials for the four redox couples 1−2 ($E°_{1,2}$), 3−4 ($E°_{3,4}$), 5−6 ($E°_{5,6}$), and 7−8 ($E°_{7,8}$) are shown in Figure 2 above the edges joining relevant reduced and oxidized species. These standard potentials are interrelated by the equilibrium constants ($K_{i,j} = a_j/a_i$) between species having the same oxidation level, $K_{1,3}$, $K_{1,5}$, $K_{3,7}$, and $K_{5,7}$ for R and $K_{2,4}$, $K_{2,6}$, $K_{4,8}$, and $K_{6,8}$ for

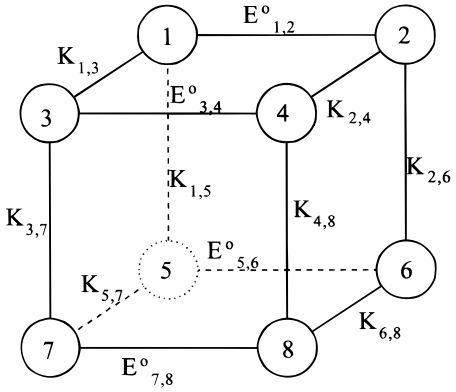

Figure 2. Cube showing a system of eight possible states, for a general ECC′ reaction. $E°$ values are shown for the 1−2, 3−4, 5−6, and 7−8 redox couples on cube edges in redox direction. Solvation equilibrium constants are shown for the 1−3, 5−7, 2−4, and 6−8 species on cube edges in the solvation direction. Reconfiguration equilibrium constants are shown for the 1−5, 3−7, 2−6, and 4−8 species on cube edges in the reconfiguration direction.

O. Each oxidation level represents a unique standard state. Consequently, the K values for the corresponding transformations of the reduced and oxidized forms will differ; these differences can be viewed as "interaction" effects arising in going from one oxidation level to another.

The relationships that exist between these $E°$ values on opposite edges of a face (1 × 1 squares) are

$$E°_{1,2} = E°_{3,4} - (RT/F)\ln[K_{1,3}/K_{2,4}] = E°_{5,6} - (RT/F)\ln[K_{1,5}/K_{2,6}] \quad (1)$$

$$E°_{7,8} = E°_{3,4} + (RT/F)\ln[K_{3,7}/K_{4,8}] = E°_{5,6} + (RT/F)\ln[K_{5,7}/K_{6,8}] \quad (2)$$

The ordering of the four standard potentials depends on the values of the equilibrium constants. No a priori constraint exists on their relative values; the latter depend on the counterion and solvent.

The effects of solvation on the $E°$ values in the top and bottom planes of Figure 2 are given by the terms $(RT/F)\ln[K_{1,3}/K_{2,4}]$ and $(RT/F)\ln[K_{5,7}/K_{6,8}]$, respectively. The effects of reconfiguration on the E° values in the front and back planes of Figure 2 are given by the terms $(RT/F)\ln[K_{3,7}/K_{4,8}]$ and $(RT/F)\ln[K_{1,5}/K_{2,6}]$, respectively.

For illustrative purposes, we consider the plausible situation of a lyophobic reduced species of configuration "a" and a lyophilic oxidized species of configuration "b". This corresponds to assuming that the equilibrium constants for R species are less than one and those for O species are greater than one. Consequently the most stable reduced species, R_a, is species 1, and the most stable oxidized species, $O^S{}_b$, is species 8 (compare Figures 1 and 2). Equations 1 and 2 show that $E°_{1,2} > E°_{3,4}$, $E°_{5,6} > E°_{7,8}$. The relative values of $E°_{3,4}$ and $E°_{5,6}$ will depend on whether the term $[K_{3,7}\,K_{6,8}]/[K_{4,8}K_{5,7}]$ is greater or less than unity. Consequently, even if the standard potentials were to be solvent independent, the solvent dependence of *all* the equilibrium constants prevents meaningful comparison of electrochemical potential data obtained with a polymer film in different solvents.

We note that the ordering of standard potentials is important in experiments involving partial redox conversion, since the ordering will determine which solvation and configuration states preferentially undergo redox conversion. This is most obvious for low overpotential experiments conducted at near-equilibrium conditions but is also pertinent to transient experiments at high overpotential. In the latter case, the "selectivity" of redox conversion will also be modulated by the standard rate constants for the variously solvated and configured couples.

Two equivalent relationships between $E°_{7,8}$ and $E°_{1,2}$ are obtained by subtracting eqs 1 and 2.

$$E°_{7,8} = E°_{1,2} + (RT/F)\ln[K_{1,5}K_{5,7}/K_{2,6}K_{6,8}] = E°_{1,2} + (RT/F)\ln[K_{1,3}K_{3,7}/K_{2,4}K_{4,8}] \quad (3)$$

Two relationships exist because interconversion of species 1 and 7, may go through either species 3 or 5,

$$K_{1,5}K_{5,7} = K_{1,3}K_{3,7} \quad (4)$$

and for the interconversion of species 2 and 8,

$$K_{2,4}K_{4,8} = K_{2,6}K_{6,8} \quad (5)$$

III.1.2. Formal Potentials. We consider the equilibrium distribution of species in Figure 1. It should be compared with Figure 2 to see the correspondence between the permselective electroactive polymer case and the general one given by eqs 1−5. The formal potential, E^f, is a key parameter for describing the composition of the film. One expression for E^f in terms of $E°_{1,2}$ is

$$E^f = E°_{1,2} + \frac{RT}{F}\ln\left(\frac{K_{2,4}K_{2,6}K_{6,8}}{K_{1,3}K_{1,5}K_{5,7}}\right) + \frac{RT}{F}\ln\left(\frac{K_{1,3} + K_{1,3}K_{5,7} + K_{1,5}K_{5,7} + K_{1,3}K_{1,5}K_{5,7}}{K_{2,4} + K_{2,4}K_{6,8} + K_{2,6}K_{6,8} + K_{2,4}K_{2,6}K_{6,8}}\right) \quad (6)$$

Analogous expressions can be obtained in terms of the three other $E°$ values (using eqs 1−5).

The unknown oxidation state dependencies of the solvation and configuration equilibrium constants make it impossible to estimate E^f a priori. A comprehensive cube model, consisting of many "microcubes" assembled into a large cube, would allow for multiple solvation and configuration states. This would give a virtually continuous distribution of $E°$ values and correspondingly more complex expressions analogous to eq 6. Such a model would allow for a molecular attribution of "interaction parameters" used in composition−potential relationships.

To rationalize modified electrode behavior, one often compares the formal potential of the monomeric solution redox species and the corresponding polymeric, surface immobilized redox species (e.g., ferrocene and polyvinylferrocene).[2,17] These E^f values commonly differ by some tens of millivolts; given the complexity of eq 6 this is not surprising. Furthermore, eq 6 shows that observed differences will be difficult to assign to specific solvation or configurational factors.

Since, by definition, the various solvation equilibrium constants will vary from one solvent to another, comparison of formal potentials for a given redox polymer in a series of solvents is a questionable exercise. Even if the solvation equilibrium constants are known, the configuration equilibrium constants will be solvent dependent. Although kinetic aspects of the redox transformation are not considered here, we note that comparison of kinetic parameters in different solvents is no more meaningful.

III.2. Effect of Counterion Concentration. We consider the redox process represented by

$$Ox^{z+}{}_{polymer} + zX^{-}{}_{polymer} + ne^{-} \rightleftarrows Red^{(z-n)+}{}_{polymer} + (z-n)X^{-}{}_{polymer} + nX^{-}{}_{soln} \quad (7)$$

where the subscripts refer to the phase in which the species resides. Our primary assumption is that there is a single, permselective polymer phase consisting of two identifiable forms, reduced and oxidized. The concentrations of these two forms are determined by the charge injected into the system. Furthermore, as stated below, the water activity does not vary with charge level. Then, at equilibrium according to the Nernst equation, the potential for the system is given by

$$E_X = E^{\circ}_X + (RT/F)\ln(\gamma_{PVF^+}\gamma_{X^-,P}/\gamma_{PVF}\gamma_{X^-,Soln}) + (RT/F)\ln[\alpha/(1-\alpha)] - (RT/F)\ln C_{X^-,Soln} \quad (8)$$

where E°_X is the standard potential in the presence of the counterion X^-, γ is the activity coefficient of the designated species at a fractional polymer oxidation level α, and $C_{X^-,Soln}$ is the concentration of the counterion in the bathing solution. The subscript P on the γ_{X^-} term indicates the polymer phase. (See the work of Buck and Vanysek for a slightly different approach to this issue.[18])

We chose the bathing solution as our reference state; consequently, the activity of the solvent does not appear in eqs 7 and 8 because it is determined by the solvent activity in the bathing solution. Since the latter is constant, so is the solvent activity in the polymer film, whatever the film's oxidation state. This will always be true at equilibrium. Under our experimental transient (nonequilibrium) conditions, departure from this situation is likely to be only minor. However, changes in mass are due to changing the solvent *concentration* in the film. These mass changes are driven by dependence of the water activity coefficient on the film's oxidation level and occur during redox interconversion. We believe that these changes that occur under nonequilibrium conditions will have only small effects on the electrode potential (see below). We stress that equilibrium is not usually achieved in a dynamic electrochemical experiment, because the time scale of the experiment is shorter than the characteristic time scale of the solvation and/or configuration changes. Note that potentiometric and gravimetric probes respond to different parameters, activity and concentration, respectively.

III.3. Transient Behavior. Two types of behavior are observed when electrochemical perturbations are imposed on an electroactive polymer film. First, a change in mass that reflects the transfer of counterions between the film and solution always occurs. This change, described by Faraday's law, is generally very rapid and is controlled either by coupled electron/counterion motion or by electrode kinetics. Motion of neutral species (solvent under permselective conditions) generates a second contribution to the mass change. This contribution can occur simultaneously and/or subsequently. If the flux of neutral species is in the same direction as the flux of counterions, the apparent molar mass ($\Delta MF/Q$) for the redox switching process will be larger than predicted by Faraday's law. Conversely, if the counterion and solvent fluxes are in opposite directions, the apparent molar mass will be less than predicted by Faraday's law; in extreme cases, the apparent molar mass may approach zero or become negative. The transient mass behavior will depend on how the solvent flux is coupled to the counterion flux and can lead to one maximum or minimum when the counterion and solvent fluxes are of opposite signs.

If the electrode is open circuited during an electrochemical experiment, then only coulostatically driven processes can occur, and a change in potential may be observed for a considerable time after open circuiting the electrode. There may be accompanying mass changes. We report results of this sort for the polyvinylferrocene (PVF) system.

Sometimes these potential and mass responses may be rationalized by slow electron-transfer kinetics with accompanying counterion transfer. Then, double-layer charge is postulated to be the source/sink of the charge required for the assumed faradaic process. The direction of double-layer discharge imposes a direction on the mass change. This rationalization fails if the mass changes oppositely to that predicted by the double-layer discharge mechanism. Then we attribute the cause of these mass changes to changes in the configuration of the polymer film.

IV. Results

IV.1. Transient Behavior. *IV.1.1. Overview.* Open circuit potentiometric and frequency measurements were done on partially oxidized PVF films immersed either in perchloric acid or sodium perchlorate solutions. The PVF film oxidation state was established by passing the required amount of charge into a film that was previously fully oxidized or reduced. Then, the PVF film oxidation state was "frozen" by opening the circuit. This prevented passing charge through the cell, without interfering with monitoring of the working electrode's potential and the crystal frequency. Because the perchloric acid and sodium perchlorate electrolyte solutions contained no redox species, the ratio of total oxidized to total reduced forms of ferrocene (each summed over all solvation and all configuration states) in the PVF film could not change during the open circuit part of the experiment.

Experiments were done on a given PVF film, using perchloric acid (0.1 and 0.01 M) and sodium perchlorate (0.1 and 0.01 M) bathing electrolytes. Five oxidation levels were established between 20% and 80% PVF^+ in perchloric acid solution and between 15% and 75% PVF^+ in sodium perchlorate solution. All the films, whatever the oxidation level, exhibited common features. Consequently, we present and discuss transient film responses in sodium perchlorate and perchloric acid bathing electrolytes at a 50% oxidation level for a representative PVF film.

If global equilibrium exists when the circuit is opened, no change in the film potential (other than an uncompensated ohmic potential drop) or in the film mass should occur. However, as is evident from Figures 3a−c and 4a−c, the PVF-coated electrode's potential and the film mass changed considerably and on different time scales. These changes of potential and mass show that the PVF film was not at equilibrium when the circuit was opened. To interpret these previously undescribed phenomena, we present the data for short times ("a" curves; tenths of a second), intermediate times ("b" curve; seconds), and long times ("c" curves; hundreds to thousands of seconds), separately.

IV.1.2. Short Time Scale (0−1 s). Figures 3a and 4a show the *E* and *M* responses at short times after opening the circuit during PVF^0 oxidation and PVF^+ reduction, respectively. The electrode potential *decreases* after opening the circuit during the anodic scan and *increases* after opening the circuit during a cathodic potential scan. The largest changes of potential, ΔE, roughly 10 mV, occur within the first 5 ms. We attribute these changes to uncompensated ohmic potential effects within the electrolyte solution and the polymer film. Mass changes on these very rapid time scales are masked by the time constant of the *f*/*V* converter in the EQCM circuitry and data acquisition rate (4 ms/point).

TABLE 1: Relaxation Mechanisms

scan direction	reaction during time (t/s) after open circuiting					
	≤0	0−0.2	0.2−1	1−5	5−2000	>2000
anodic	1→2 (+Q) 5 → 6 (+Q)	2 → 4 → 8 (+M, −E) 2 → 6 → 8 (−E, +M) 6 → 8 (+M)	2 → 6 (−E) 4 → 8 (−E) 5 → 1 (−E)	2 → 6 (−E) 3 → 1 (−M) 7 → 5 (−M)	3→ 1 (−M) 7 → 5 (−M) 2 → 1 (−Q) 5 → 6 → 8 (+Q, +M)	3→ 1 (−M) 7 → 5 (−M)
cathodic	8→7 (−Q)	7 → 3 → 1 (+E, −M) 7 → 5 → 1 (−M, +E)	5 → 1 (+E)	3 → 1 (−M)	3 → 1 (−M) 6 → 8 (+M)	3 → 1 (−M)

These initial, very rapid potential changes are followed, in the interval 5−1000 ms, by continued, slower potential changes in the initial directions. At 200 ms it was about 30 mV in the anodic scan and 15 mV in the cathodic scan. At 1000 ms it was about 40 mV in the anodic scan and 25 mV in the cathodic scan. The film mass changed by ca. 5 ng, over the first 1000 ms, mostly within the first 200 ms. For anodic scan experiments we observed an increase in the film's mass and for cathodic scan experiments a decrease in the film's mass. Analogous response patterns were observed for experiments (not shown) involving open circuiting films at different stages of redox conversion.

IV.1.3. Intermediate Time Scale (1−25 s). In both the anodic and cathodic scan experiments (Figures 3b and 4b) the electrode potentials continue their slow changes, but in opposite directions for the two experiments, toward almost constant values. Remarkably, the film mass transients do not show this "mirror-image" response. Rather, both showed a decrease until about 5 s, following which both increase slowly by 4 ng over the next 20 s. Interruption experiments at all charge levels, and in both scan directions, exhibited a mass minimum at times in the range 5−10 s.

IV.1.4. Longer Times (25−3600 s). Throughout this interval and for both scan directions, the electrode potential shifts to more positive values; these changes are about a few millivolts. Over the interval 25−1500 s both mass transients are similar, showing an increase of about 30 ng. Subsequently, the mass transients differ: for the cathodic scan the mass continues to increase, although very slowly, but for the anodic scan the mass reaches a maximum and then decreases by a few nanograms.

V. Discussion

We will first present our mechanistic diagnosis of the transient E and M data using the scheme of cubes. Interestingly, this leads to a situation in which solvent both enters and leaves the film on different time scales; we term this "ebb and flow". Finally, we consider and reject an alternative mechanistic explanation.

Our interpretation of transient EQCM responses is based upon the following characteristic signatures of the three elementary steps. Redox state changes cause changes in E, Q, and M. Solvation changes are associated predominantly with changes in M although they may cause small potential changes. Configuration state changes are associated only with changes in E. Since the redox state is "frozen" at a charge level, Q, in the present experiments, we use the E and M responses as diagnostics for the occurrence of configuration and solvation steps, respectively. We recognize that complete step separations may not always occur in a real system; nevertheless, these diagnostics allow identifying the dominant process during a transient.

V.1. Assignment of Elementary Steps. The mechanism that we ultimately arrived at is shown in Table 1. Referring to this table may be helpful as we present our analysis of the data.

TABLE 2: Electrode Potential and Film Mass Changes for PVF in 0.01 M $HClO_4$ after 1 h at an Open Circuit[a]

anodic scan data			cathodic scan data		
fraction oxidized[b]	E_{1hr} [mV][c]	ΔM_{1hr} [ng][d]	fraction oxidized	E_{1hr} [mV]	ΔM_{1hr} [ng]
0.1511	291.7	107.8	0.1939	294.5	178.5
0.3025	318.5	236.6	0.3289	315.5	213.5
0.4476	332.6	249.0	0.4620	327.7	256.9
0.6054	348.7	345.1	0.6046	344.3	345.1
0.7452	371.7	423.5	0.7446	368.7	394.5

[a] Mass data are referred to a completely reduced film. [b] Fraction of oxidized ferrocene sites. [c] E_{1hr} = electrode potential (vs SCE) after 1 h at an open circuit. [d] ΔM_{1hr} = difference between film mass after 1 h at an open circuit and film mass of the fully reduced film during the cycling.

The potential and mass changes seen shortly after open circuiting the electrode (see Figures 3 and 4) prove that equilibrium does not exist at times less than 3600 s. The mass and potential transient over the experiment for both the anodic and cathodic experiments show that both solvation and reconfiguration processes are occurring. We now propose to separate contributions of these processes and to identify at what times they occur during the open circuit phase of our experiments.

V.1.1. 0 s ≤ t ≤ 0.2 s. In our theoretical exposition, our model merely required all $K_{i,j}$ values for one redox state to be less than one and for the other redox state to be greater than one. The data allow us now to be more specific. First, we can say the $K_{i,j}$ values for the oxidized species are greater than one. Second, from the size of the total potential change at open circuit (compare Figures 3 and 4) we can estimate the overall free energy changes associated with solvation and polymer reconfiguration. The total potential change after opening the circuit at 50% redox conversion, i.e., the difference in $E°$ values, is ca. 100 mV. This corresponds to $\Delta G° \approx 10$ kJ mol^{-1} or a product of solvation and reconfiguration equilibrium constants $K_{2,4}\,K_{4,8} = K_{2,6}\,K_{6,8} \approx 30$.

To estimate the effect of transient water content on the open circuit potential, we need to know what fraction of film's water content has been achieved then. The data in Table 2 and Figure 3 allow us to do this. We calculate that the total solvent population change (from the fully reduced film to the 50% oxidized film) 1 h after an open circuit is 5.4 mol of water per mole of ferrocene sites oxidized. During the potentiodynamic part of the experiment (from the fully reduced state to an open circuit), the water content of the film increases only by 3.1 mol of water per mole of ferrocene sites oxidized. This leaves 2.3 mol of water per mole of ferrocene sites (previously) oxidized to be transferred following an open circuit. The mass change in the 300 ms following an open circuit corresponds to a water content increase of ca. 0.6 mol of water per mole of ferrocene sites oxidized. Since the experiment is not very far from equilibrium, we assume that the Nernst equation will give a reasonable approximation to the solvent-related potential

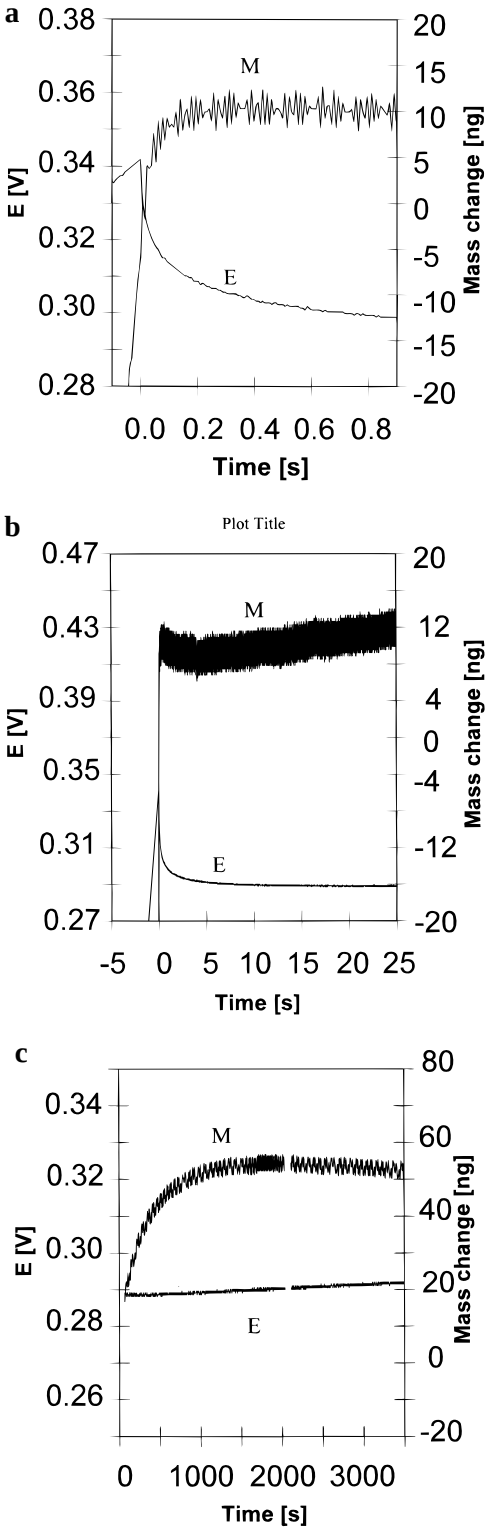

Figure 3. Potential and film mass change behavior of a PVF film (Γ = 12.0 nmol cm^{-2}) in 0.01 M $HClO_4$ after opening of the circuit during an anodic potential scan at 50 mV s^{-1}. The fraction of oxidized redox sites = 50%; (a) short time scale, (b) intermediate time scale, (c) long time scale.

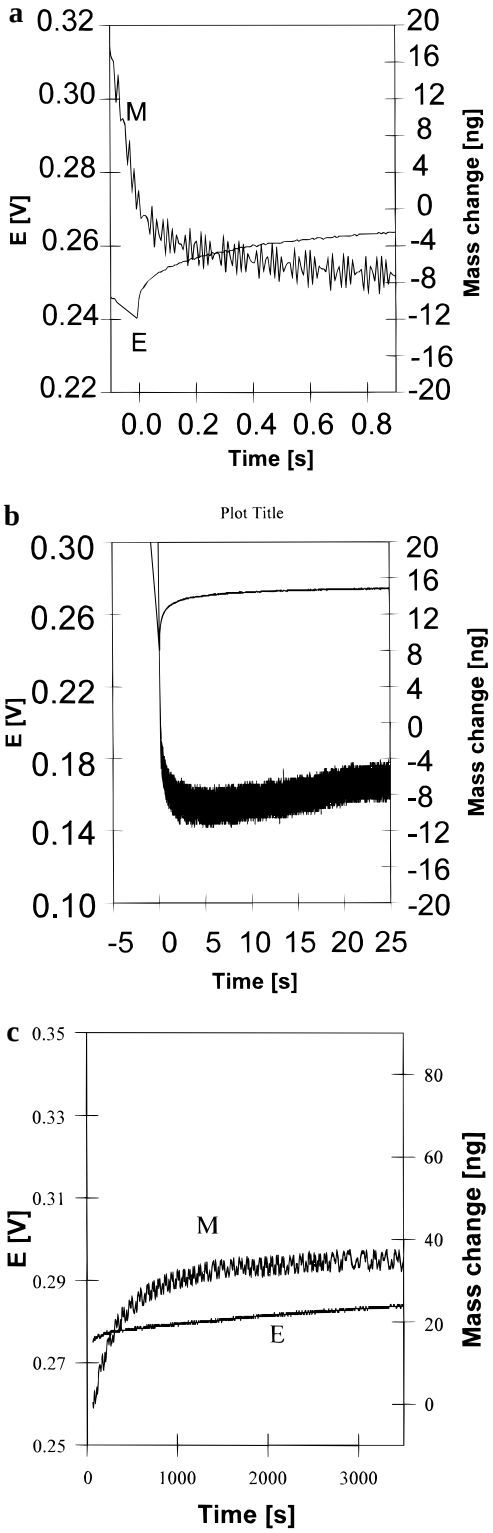

Figure 4. Potential and film mass change behavior of a PVF film (Γ = 12.0 nmol cm^{-2}) in 0.1 M $HClO_4$ after opening of the circuit during a cathodic potential scan at 50 mV s^{-1}. The fraction of oxidized redox sites = 50%; (a) short time scale, (b) intermediate time scale, (c) long time scale.

transient. This predicts a 59β millivolt per decade slope, where β is the stoichiometric coefficient for water transfer at the 50% oxidation level. Our data give $\beta \approx 3$ at an open circuit, from which we calculate a potential transient over the interval 0−300 ms of ∼13 mV. The observed potential change over this time, ∼35 mV, is much larger. We therefore deduce that a polymer reconfiguration also is occurring besides solvation.

V.1.2. 0.2 s ≤ t ≤ 1 s. In the anodic scan experiment, the potential transient at constant mass over the interval 200−1000 ms shows purely configurational changes. In the cathodic scan experiment, besides a potential transient, small mass changes occur during this time. This result suggests polymer reconfiguration, with concurrent solvent level changes. It is unlikely that the latter are sufficient to account for the observed potential

changes because of the weak dependence of the electrode potential on solvent content (see above).

V.1.3. 1 s ≤ t ≤ 5 s. Before the mass minima in Figures 3b and 4b, there are continued potential changes only in the anodic scan experiment, suggesting ongoing polymer reconfiguration. The associated mass (solvent) changes in this time regime are unusual in that these transients are similar (in the same directions) despite the different directions of approach to the 50% oxidation level. After the mass minima, potential changes are much smaller. Although a quantitative interpretation of the shape of the potential transient is beyond the scope of this paper, the long tail suggests a distribution of relaxation times; this could be accommodated within our model by multiple cubes in the "*z*" direction. The switch from dominance by potential to mass (loss) changes implies a switch from reconfiguration to (de)-solvation control. Interestingly, both the anodic and cathodic potential scans generate solvent deficient intermediate states.

V.1.4. 5 s ≤ t ≤ 3600 s. At much longer times (see the second parts of Figures 3b and 4b and all of Figures 3c and 4c) mass changes dominate. In both cases the solvation processes described in the previous paragraph "overshoot" slightly, evidenced by broad maxima at ca. 1700 s (anodic scan) and 2500 s (cathodic scan). The small concurrent potential changes might be associated with reconfiguration (see above) or the minor Nernstian response to solvent population changes in the film.

The complex mass behavior during the entire experiment, at fixed total charge, is a consequence of (1) population redistributions among oxidized and reduced states, (2) changing solvent level, and (3) reconfiguration. The oscillatory behavior suggests the system to be nonlinear. Our cube model is intrinsically a 3-D representation of a nonlinear system. We now explore the observed "ebb and flow" of solvent in these terms.

V.2. Ebb and Flow of Solvent. The occurrence of extrema in the mass/time curves under open circuit conditions is a unique result. Extrema represent a reversal of solvent transfers to and/or from the film. This situation requires sequential conversion of (at least) three species that have different solvation levels. If an intermediate species has the highest solvation level, a maximum in mass will occur. If the intermediate has the lowest solvation level, a mass minimum will be found.

The potential responses on open circuiting were monotonic. During oxidation, the potential transient was in a negative direction for the entire experiment. From our discussion of eqs 1 and 3, we see that this implies that oxidized species on the upper plane of the cube in Figure 2 convert to oxidized species on the lower plane, i.e., species 2 converts to 6 and/or species 4 then 8. The same direction of potential change would be observed if reduced species on lower plane of the cube in Figure 2 convert to reduced species on the upper plane, i.e., species 5 converted to 1 and/or species 7 converted to 3.

In Table 1, we show a mechanism that accounts for the experimental potential (*E*) and mass (*M*) changes in terms of reconfiguration and solvation processes. Although open circuit conditions prevail, charge (*Q*) redistribution processes within the various species are still possible because the formal potentials of differently solvated or configured couples are dissimilar.

During the anodic experiment, a combination of solvation equilibria (which favors unsolvated reduced states) and film history (originating in reduced forms) favors species 1 and 5 as the primary reduced species on the reduced face of the cube. However, we also allow for the existence of secondary reduced states, 3 and 7. The latter two states are assumed to be less populated than states 1 and 5 and kinetically slow to change solvation, configuration, and oxidation levels.

Before open circuiting the electrochemical process is dominated by conversion of species 1 and 5 to 2 and 6, respectively. The experiment of Figure 3 monitors the way in which these intermediate species relax to the dominant product, species 8. A detailed explanation for the time course of the observed potential and mass excursions is given in Table 1. Qualitatively, conversions of species 2 and 6 to 8 on the product (oxidized) face of the cube generates negative potential and positive mass changes. Replenishment of the depleted species 1 and 5 by 3 and 7 on the reactant (reduced) face of the cube subsequently generates negative mass and continued negative potential changes; the desolvation steps are sufficiently slow to persist until the end of the experiment.

The generation of species 5 favors the production of 6, a redox conversion. Under coulostatic conditions this requires an equivalent reduction process. The latter can only be the conversion of species 2 to 1, since $E^\circ_{1,2}$ is the only redox potential more positive than $E^\circ_{5,6}$ (see eqs 1 and 2). This interconversion around the back face of the cube is analogous to a corrosion reaction: effectively species 2 oxidizes 5, producing 1 and 6. Regeneration of species 6 leads to a solvent ingress ($6 \rightarrow 8$) superimposed on the desolvation steps described above. This ingress is seen experimentally, peaking at 1700 s.

The corresponding mechanistic rationalization for the cathodic scan is shown in the lower half of Table 1. The justification for the table entries follows analogous arguments to those presented above for the oxidation scan. Although a detailed exposition is unwarranted, some observations are necessary. First, the predominant "reactants" in the cathodic experiment are species 8 and 6, which have the same configuration. Our interpretation of the experimental results requires that the reduction of species 6 to 5 to be slower than that of species 8 to 7. A microscopic explanation might be that counterion motion within a less solvated region is hindered. In addition, on the basis of interpretation of the anodic experiment, we assume that the solvation step 6 to 8 must be relatively slow. Second, the similarity of the mass responses for the both anodic and cathodic scans at $t > 1$ s are reflected in similar processes: a background desolvation of species 3 to 1 with solvation of species 6 to 8 is common to both mechanisms. Third, solvent entry into the film, via solvation of species 6, arises for different reasons in the two experiments. In the anodic experiment it is due to species 5 being the major reduced species oxidized (to 6) before opening the circuit. In the cathodic scan, consideration of standard potentials suggests that species 6 should be reduced more readily than species 8. However, our mechanism (Table 1) requires that species 6 persist until long times (to act as a solvent sink). The survival of species 6 is a consequence of the rapid production of its redox partner 5 by the $8 \rightarrow 7 \rightarrow 5$ route. The common feature of both experiments is a high population of species 5; species 6 is depleted via solvation to species 8 in both cases.

V.3. Alternative Hypothesis. We see from Figures 3a and 4a that an overpotential exists at the PVF-filmed electrode. Coulostatic discharge of this overpotential might explain the observed potential changes; i.e., the oxidation/reduction of the film may continue by (dis)charging the double layer. This mechanism requires that the mass increase when the electrode potential becomes more positive (counterion incorporation during film oxidation when the double layer functions as an oxidant). The coulostatic mechanism also requires a mass decrease when the electrode potential becomes more negative

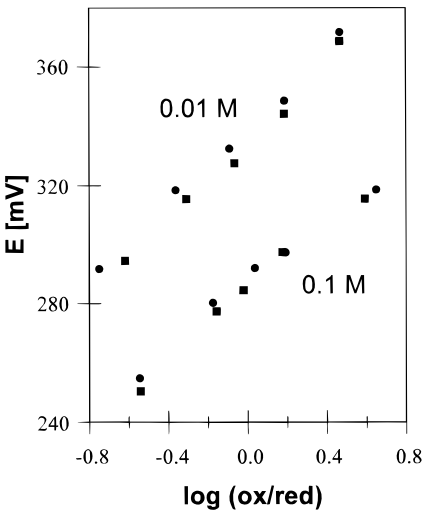

Figure 5. *E* vs log(ox/red) for a PVF film ($\Gamma = 12.0$ nmol cm^{-2}) in $HClO_4$ solutions 1 h after establishing an open circuit. Upper curves are 0.01 M solutions and lower curves are 0.1 M solutions: anodic potential scan data (■); cathodic scan data (●). Potential scanned at 50 mV s^{-1} before establishing an open circuit.

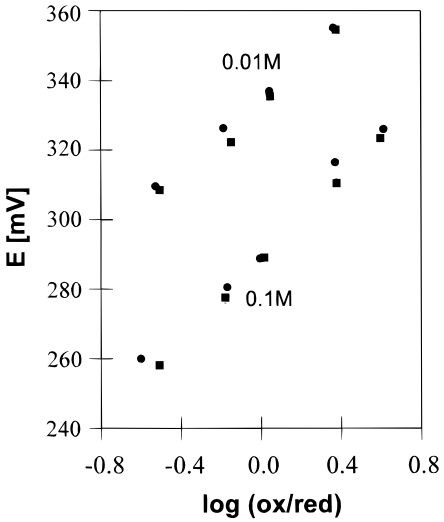

Figure 6. *E* vs log(ox/red) for a PVF film ($\Gamma = 12.0$ nmol cm^{-2}) in $NaClO_4$ solutions 1 h after establishing an open circuit. Upper curves are 0.01 M solutions and lower curves are 0.1 M solutions. Anodic potential scan data (■); cathodic scan data (●). Potential scanned at 50 mV s^{-1} before establishing an open circuit.

(counterion expulsion when the double layer functions as a reductant). These predictions are exactly the opposites to the experimental results in Figures 3a and 4a. Consequently, we reject this explanation for these PVF experiments, although another system might show such behavior.

V.4. Redox "Thermodynamics" of PVF Approaching Equilibrium. *V.4.1. Nernst Plot.* Values of the electrode potential and electrode mass after 3600 s at an open circuit are listed in Tables 2−4 for perchloric acid and sodium perchlorate bathing electrolytes. The open circuit potentials after 1 h for the anodic scan and cathodic scan experiments are in good agreement. They yield Nernst plots (Figures 5 and 6) which are shifted from each other by only a few millivolts for the anodic and cathodic scan data. Their slopes (Table 4, "*B* values") are in reasonable agreement with the theoretical ones, as would be expected for a film that was totally permselective with respect to perchlorate ions.[19,20] The difference (4−8 mV) between the anodic and cathodic scan formal potentials (Table 4, "*A* values") is evidence that equilibrium has not been established even after 1 h at an open circuit. Despite this observation, the predicted difference in formal potentials of 59 mV (eq 7) between the 0.01 and 0.1 M solutions is somewhat higher than the observed values. Our results show a smaller deviation from Nernstian behavior for PVF than reported previously.[6,7] We believe this is caused by differences in film history and experimental conditions.

TABLE 3: Electrode Potential and Film Mass Changes for PVF in 0.1 M $HClO_4$ after 1 h at an Open Circuit[a]

anodic scan data			cathodic scan data		
fraction oxidized[b]	E_{1hr} [mV][c]	ΔM_{1hr} [ng][d]	fraction oxidized	E_{1hr} [mV]	ΔM_{1hr} [ng]
0.2217	254.9	150.5	0.2234	250.5	178.5
0.4009	280.3	238.0	0.4105	277.4	250.6
0.5211	292.1	283.5	0.4877	284.6	270.2
0.6084	296.4		−0.6001	297.5	331.2
0.8166	318.7		−0.7959	315.6	

[a] Mass data are referred to a completely reduced film. [b] Fraction of oxidized ferrocene sites. [c] E_{1hr} = electrode potential (vs SCE) after 1 h at an open circuit. [d] ΔM_{1hr} = difference between film mass after 1 h at an open circuit and film mass of the fully reduced film during the cycling.

TABLE 4: (RT/nF) and E' Values for PVF Films in $HClO_4$ and $NaClO_4$ Solutions[a]

	B		A [mV]	
system	anodic[b]	cathodic[c]	anodic	cathodic
0.01 M $HClO_4$	64 ± 3	67 ± 4	340 ± 4	332 ± 6
0.1 M $HClO_4$	66 ± 4	67 ± 1	288 ± 4	284 ± 1
0.01 M $NaClO_4$	51 ± 2	53 ± 4	338 ± 3	331 ± 8
0.1 M $NaClO_4$	57 ± 3	59 ± 1	292 ± 4	288 ± 2

[a] Best fits of Nernst plots to $E = A + B$ log(ox/red). [b] Anodic = anodic scan data. [c] Cathodic = cathodic scan data.

The close approach to Nernstian behavior supports the view that the partially oxidized PVF film is a single phase in which the amounts of totally reduced and totally oxidized species are determined by the charge injected into the film. The insensitivity of the activity coefficient term in eq 8 to the oxidation level is very interesting. One might expect, by analogy with aqueous electrolyte theory, that there could a substantial change in this ratio of activity coefficients with ionic strength as charge was introduced or withdrawn from the film. This change would manifest itself through a substantial deviation from the theoretical Nernstian slope of 59 mV/decade. One possible rationalization of this situation would be that the counterions in the film are ion-paired to the charge centers. As shown in the next section, this leads to a plausible explanation of the relatively close agreement between experiment and theory.

V.4.2. Ion-Pair Model. If we assume that the oxidized PVF is ion-paired to the counteranion ($Ox^+X^-_{polymer}$), the half-reaction eq 7 for PVF and a monovalent anion becomes

$$Ox^+X^-_{polymer} + e^- \rightleftarrows Red_{polymer} + X^-_{soln} \qquad (9)$$

Then, the potential for the system is given by

$$E_X = E^\circ_X + (RT/F)\ln(\gamma_{PVF^+X^-,P}/\gamma_{PVF}\gamma_{X^-,Soln}) + (RT/F)\ln[\alpha/(1-\alpha)] - (RT/F)\ln C_{X^-,Soln} \qquad (10)$$

where $\gamma_{PVF^+X^-,P}$ is the activity coefficient of the ion-paired, oxidized form of PVF. The ion-paired activity coefficient should behave similarly to that of a neutral species. Thus, it and the uncharged PVF activity coefficient should change minimally with oxidation level. Therefore, the ratio of the

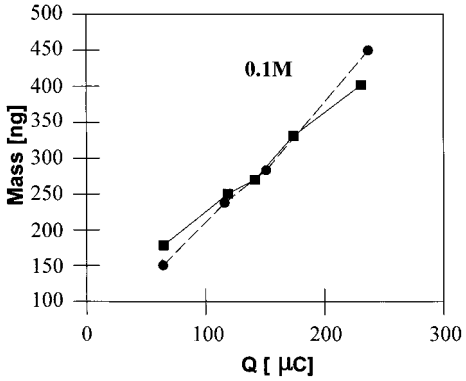

Figure 7. Mass vs charge curve for a PVF film ($\Gamma = 12.0$ nmol cm^{-2}) in 0.1 M $HClO_4$ 1 h after establishing an open circuit: anodic potential scan data (■); cathodic scan data (●). Potential scanned at 50 mV s^{-1} before establishing an open circuit.

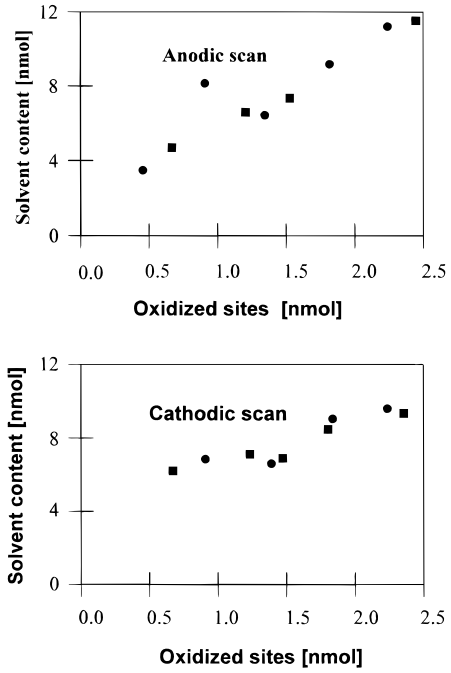

Figure 8. Solvent content vs amount of oxidized redox sites curve for a PVF film ($\Gamma = 12.0$ nmol cm^{-2}) in $HClO_4$ solutions 1 h after establishing an open circuit. Potential scanned at 50 mV s^{-1} before establishing an open circuit. 0.01 M data (●); 0.1 M data (■). Top is anodic potential scan, and bottom is cathodic potential scan.

activity coefficients for the ion pair and the uncharged redox site should change minimally with redox composition. Thus, in a bathing solution of constant composition, it is understandable that a plot of E vs $\ln[\alpha/(1 - \alpha)]$ should have a near-Nernstian slope.

V.4.3. Temporal Variation of Water Content. For perchloric acid solutions, Figure 7 presents the total mass change data as a function of charge obtained during cathodic and anodic potential scan experiments after 1 h at an open circuit. The amounts of water in the film for 0.1 and 0.01 M perchloric acid experiment were found using Faraday's law to calculate the mass of counterions in the film and subtracting it from the observed film mass (see Figure 7). The mass of water in the film after 1 h at an open circuit varies with the oxidation level. Figure 8 presents these data as plots of nanomoles of solvent vs nanomoles of ferrocinium sites. These plots show that, even after 1 h at an open circuit, the film had not reached solvent content equilibrium. (The cathodic and anodic scan data do not coincide.) Agreement between the anodic and cathodic scan

TABLE 5: Comparison Estimates of E^f Obtained by Different Approaches[a]

system	$(E_p^a + E_p^c)/2$ [mV]	$(E_{q/2}^a + E_{q/2}^c)/2$ [mV]	$E_{50\%}^a$ [mV]	$E_{50\%}^c$ [mV]
0.01 M $HClO_4$	328.8	345.0	340.0	334.0
0.10 M $HClO_4$	280.0	292.5	290.0	286.0
0.01 M $NaClO_4$	345.0	367.5	337.0	335.0
0.10 M $NaClO_4$	296.0	312.5	286.0	289.0

[a] E_p^a = anodic peak potential; E_p^c = cathodic peak potential; $E_{q/2}^a$ = potential of half charge in anodic scan; $E_{q/2}^c$ = potential of half charge in cathodic scan; $E_{50\%}^a$ = open circuit potential after 1 h, 50% oxidation, anodic scan; and $E_{50\%}^c$ = open circuit potential after 1 h, 50% oxidation, cathodic scan. The scan rate used in cyclic voltammetry was 50 mV s^{-1}.

experiments was best at intermediate oxidation levels. To a first approximation, the water content is a linear function of the film's oxidation level. For the anodic and cathodic scans, respectively, the slopes of the data in Figures 8 are ~4 and ~2 mol of water/mol of ferricinium. The differential nature of the mass measurement prevents making accurate absolute comparisons of water content. However, the changes of the films' water content with oxidation level are greater during the anodic scan. The mass responses in Figures 3c and 4c both show that desolvation is still occurring at long times; i.e., in their approach to equilibrium from either fully oxidized or fully reduced states the films are solvent-rich.

Potentials measured at a 50% oxidation level correspond to the formal electrode potential, E^f. In principle, for a simple electron-transfer situation and for which the transfer coefficient is ~$^1/_2$, E^f can be derived from three kinds of measurements: (i) by averaging cyclic voltammetric anodic and cathodic peak potentials whose average is independent of scan rate, (ii) by averaging potentials corresponding to 50% oxidation in a cyclic voltammetric experiment, and (iii) by averaging open circuit potentials at 50% conversion for cathodic and anodic scan experiments. Table 5 gives these data for PVF films exposed to the perchloric acid and sodium perchlorate solutions we used. The scan rate used in the cyclic voltammetric experiments was 50 mV s^{-1}. The "equilibration" time for the open circuit experiments was 1 h.

The E^f estimations, provided by the cyclic voltammetric and coulometric approaches (Table 5), differ. The mean values of the formal potentials obtained in our cathodic and anodic scan experiments (columns four and five of Table 5) agree with each other and with columns four and five, respectively, of Table 4. This agreement reflects the similar, long time scales of these coulometrically based experiments.

We summarize the data in Tables 4 and 5 as follows. The time scale of the experiment affects the calculated value of E^f. Only the long time scale experiments yield self-consistent results; we believe the open circuit data best represent the correct E^f values. The shorter time scale (voltammetric) measurements are not self-consistent.

The requirements that "kinetic averages" obtained from cyclic voltammetric and other cyclic experiments correspond to a thermodynamic result are very stringent: the transfer coefficient for electron transfer must be 0.5, and there can be no coupled chemical steps pre- or post-electron transfer. These conditions are not met even by a scheme of squares kinetic model, let alone a scheme of cubes model. We note that all the potentiodynamic results reported here correspond to (very) nonequilibium conditions. Consequently, any agreement between them and the open circuit formal potentials can only be accidental. Of the methods used, the open circuit potential technique will most closely ap-

proximate the equilibrium result, since the experimental time scale is the longest. We cannot recommend conventional cyclic voltammetric experiments for determining E^f values.

The differences in water content seen for the data in Figure 8 show that the system we studied was not at thermodynamic equilibrium. Still, the formal potentials obtained by our open circuit approach differed only by a few millivolts. Also, the formal potentials showed nearly Nernstian response as judged by the films' dependence on counterion concentration in the supporting electrolyte, and the classical Nernst plot gave a slope near 59 mV/decade. The observed near-Nernstian behavior arises because the system was not far from equilibrium, where the above-mentioned kinetic complications were much smaller.

VI. Conclusions

Partial redox switching of PVF films under permselective conditions in aqueous perchlorate bathing electrolytes produces films that reach equilibrium very slowly. The relaxation kinetics involve polymer reconfiguration and solvent (water) transfer. The relative rates of polymer reconfiguration and solvation vary with the time following the imposition of coulostatic conditions. Initially, the two rates are comparable; next relaxation dominates, then both are comparable again, and finally solvation controls. Transient mass and open circuit potential responses, reflecting solvation and polymer configuration changes, can be rationalized within the "scheme of cubes". Among other phenomena, the scheme of cubes predicts multiple solvation steps, which lead to the possibility of extrema in solvent populations; this prediction was confirmed.

Even after an hour at an open circuit, the film is still exchanging small amounts solvent with the bathing electrolyte. These transfers are reflected primarily in the film mass and do not affect open circuit potentiometric measurement. Thus, a near-Nernstian relationship exists between the polymer modified electrode potential and the extent of polymer oxidation for a film allowed to equilibrate for 1 h in the bathing electrolyte.

Acknowledgment. This work was supported by the National Science Foundation through Grants CHE-91-15462 and CHE-96-16641.

References and Notes

(1) Murray, R. W. In *Electroanalytical Chemistry* Bard, A. J., Ed.; Marcel Dekker: New York, 1984; Vol. 13.
(2) Hillman A. R. In Linford, R., Ed. *Electrochemical Science and Technology of Polymers*; Elsevier Applied Science Publishers: London, 1987; p 103.
(3) Alcacer, L., Ed. *Conducting Polymers, Special Applications*; Reidel: Dordrecht, 1987.
(4) Skotheim, T. A., Ed. *Handbook of Conducting Polymers*; Marcel Dekker: New York, 1986; p 97.
(5) Dautartas, M. F.; Evans, J. F. *J. Electroanal. Chem.* **1980**, *109*, 301.
(6) Dautartas, M. F.; Bowden, E. F.; Evans, J. F. *J. Electroanal. Chem.* **1987**, *219*, 71.
(7) Bowden, E. F.; Dautartas, M. F.; Evans, J. F. *J. Electroanal. Chem.* **1987**, *219*, 91.
(8) Peerce, P. J.; Bard, A. J. *J. Electroanal. Chem.* **1980**, *114*, 89.
(9) Martin, C. R.; Rubinstein, I.; Bard, A. J. *J. Am. Chem. Soc.* **1982**, *104*, 4817.
(10) Lang, G.; Bacskai, J.; Inzelt, G. *Magyar Kemiai Folyoirat* **1990**, *96*, 263.
(11) Hillman, A. R.; Bruckenstein, S. *Faraday Trans.* **1993**, *89*, 339.
(12) Hillman, A. R.; Bruckenstein, S. *Faraday Trans.* **1993**, *89*, 3779.
(13) De Gennes, P. A. *Macromolecules* **1981**, *14*, 1637.
(14) Hillman, A. R.; Loveday, D. C.; Bruckenstein, S. *Langmuir* **1991**, *7*, 191.
(15) Bruckenstein, S.; Shay, M. *Electrochim. Acta* **1985**, *30*, 1295.
(16) Bandey, H. L.; Gonsalves, M.; Hillman, A. R.; Glidle, A.; Bruckenstein, S. *J. Electroanal. Chem.* **1996**, *219*, 410.
(17) Murray, R. W., Ed. *Molecular Design of Electrode Surfaces*; Wiley: New York, 1992.
(18) Buck, R. P.; Vanysek, P. *J. Electroanal. Chem.* **1990**, *290*, 73.
(19) Hillman, A. R.; Loveday, D. C.; Bruckenstein, S. *J. Electroanal. Chem.* **1989**, *274*, 157.
(20) Pater, E.; Bruckenstein, S.; Hillman, A. R. *Faraday Trans.* **1998**, *94*, 217.